ICARUS **122,** 92–106 (1996)
ARTICLE NO. 0111

Spectrophotometry and Organic Matter on Iapetus

2. Models of Interhemispheric Asymmetry

PETER D. WILSON AND CARL SAGAN

Laboratory for Planetary Studies, Cornell University, Ithaca, New York 14853-6801
E-mail: wilson@astrosun.tn.cornell.edu

Received March 2, 1995; revised December 19, 1995

The albedo asymmetry of Iapetus is unique in the Solar System. Many models have been proposed to explain why the leading hemisphere has a reflectance 10–20 times lower than the trailing hemisphere and the poles. Compositional and observational constraints appear to rule out many of these models. Little attempt has been made to explain why, of all the moons in the Solar System, only Iapetus displays such properties. The photometric differences between Phoebe and the dark material on Iapetus, and the expectation that accreted dust from Phoebe would darken the poles more than the antapex of orbital motion on Iapetus, make the Phoebe dust model inconsistent with observations. Other models that instead have Iapetus accreting circumsaturnian material coming from either Hyperion or Iapetus itself are also beset by an inability to explain the bright poles. The endogenous extrusion of dark organics, by itself, is ruled out, since it is extremely unlikely that this model would produce elliptical albedo contours centered on the apex of orbital motion. The modern impact flux does not deliver enough kinetic energy to Iapetus's surface to vaporize significant quantities of water ice and produce a lag deposit. Also, impact vaporization is expected to form a similar lag deposit on the trailing hemisphere. Our most optimistic estimate of the amount of organic material that accumulates on the surface from *in situ* radiation synthesis of solid organics from methane clathrate is more than sufficient to explain the albedo and spectrum. This process, however, is more effective on the trailing than leading hemisphere, so the reverse asymmetry is expected.

Iapetus's asymmetry is best explained by a thick primordial low-albedo subsurface layer of organics exhumed by impact erosion. The layer may be the consequence of ancient thermochemistry in Iapetus's interior, processing methane and/or HCN into dark organic matter which was then extruded over the entire surface. The model requires a thin layer of nearly pure water ice, either exogenous or endogenous, deposited over the dark organics. Subsequent impacts would have preferentially eroded the ice on the leading hemisphere, revealing the underlying dark material. The uniqueness of Iapetus's albedo asymmetry can be understood by its impact-induced erosion rate, size, and formation distance from the Sun and Saturn—a combination of parameters duplicated nowhere else in the Solar System. Tests of these conclusions can be made by Cassini.
© 1996 Academic Press, Inc.

INTRODUCTION

The albedo asymmetry of Iapetus has been known since shortly after its discovery (Cassini 1676). The Voyager missions revealed a surface with a visible reflectance of 2–3% at the apex of motion, ~30% at the antapex, and ~50% at the poles (Squyres *et al.* 1984). This is the greatest albedo range known of any object in the Solar System (Squyres *et al.* 1984). The unique nature of Iapetus has been a major mystery to astronomers for over 300 years.

Several models have been proffered to explain the albedo asymmetry, listed here in chronological order: (a) preferential impact erosion by cometary debris of a thin veneer of ice on the leading hemisphere, revealing underlying dark silicates (Cook and Franklin 1970); (b) coating of the leading hemisphere by dark matter impact-ejected from nearby Phoebe (Soter 1974); (c) preferential endogenous extrusion of organic matter onto the leading hemisphere (Smith *et al.* 1982); (d) production of a lag deposit of an indigenous dark surface component by impacting dust preferentially vaporizing the ice in the leading hemisphere (Cruikshank *et al.* 1983); (e) synthesis of organic solids by ultraviolet irradiation of methane-rich ice and the subsequent ballistic redistribution of surface material in response to the impact flux gradient (Squyres and Sagan 1983); (f) the reaccretion of ejecta following a large cometary impact (Tabak and Young 1989); and (g) the accretion of material coming from the disruption of Hyperion by a large comet impact (Matthews 1992). Processes (a), (d), and (e) all involve impact by interplanetary debris, and all predict (cf. Cook and Franklin 1970) similar photometric contours of the Iapetus dark material. The predicted contours are similar to those observed (Squyres and Sagan 1983). It seems fair to say that none of these mechanisms has gained widespread acceptance. Some analyses propose

0019-1035/96 $18.00
Copyright © 1996 by Academic Press, Inc.
All rights of reproduction in any form reserved.

a mix of endogenous and exogenous sources (e.g., Smith *et al.* 1982).

In the following section we review what is known of the composition of Iapetus's surface. We then outline the major characteristics of the albedo pattern and draw inferences about the physical and chemical processes at work on Iapetus. Finally, we confront each model for the albedo asymmetry with the derived constraints.

COMPOSITION MODELS

The bright material is very nearly pure water ice (Clark *et al.* 1984). From Voyager photometry it has an orange to violet ratio (OR/VI) of 1.25 (Squyres *et al.* 1984), requiring a red contaminant also to be present. Since the dark material on the leading hemisphere has an OR/VI of 1.45 (Squyres *et al.* 1984), the contaminant is likely to be identical to the dark material but diluted by higher concentrations of water ice. In going from bright region to dark region, both the albedo and the color change in a remarkably smooth and continuous manner (Buratti and Mosher 1995), indicating a similar smooth gradient in the concentrations of water ice and dark material. The albedo extremes occur at the apex and near the poles, at which points the water ice concentration is, respectively, at its lowest and highest. The red contaminant may be emplaced (or exposed) either by the same mechanism which produced the dark apex, but with an efficiency that follows the albedo/color contours, or by secondary means such as the deposition of impact ejecta from an already darkened leading hemisphere.

Bell *et al.* (1985) have taken visible and near-infrared spectra of the leading and trailing hemispheres of Iapetus and derived a spectrum of pure dark material. They model this spectrum with a 10% organic and 90% hydrated silicate mixture. For the organics, they attempted to simulate Murchison organic residue but produced a material that was brighter than real Murchison at 0.7–1.3 μm. It is at these wavelengths that their model is a poor match to the spectrum, but it is a good fit at the other wavelengths in the range 0.5–2.4 μm.

We have applied Hapke reflectance theory to the Bell *et al.* derived spectrum of the Iapetus dark material, using water ice and five types of organic solids as candidate surface materials (Wilson and Sagan 1995). Out of 18 million models searched, an intraparticle mixture of poly-HCN, Murchison organic residue, and water ice (henceforth abbreviated H, M, and W) produces a very good match to the derived spectrum (Wilson and Sagan 1995). The other organic materials considered were kerogen, ice tholin (from irradiated hydrocarbon/water ice mixtures), and Titan tholin (henceforth abbreviated K, I, and T). Particle and areal mixtures were also considered. Ice tholin replacing water ice in the HMW model provides the second best combination and is fully acceptable within the combined errors of measurement. Particle and areal mixtures of HTI and HTM also provide very good fits. Although Titan tholin is produced in an atmosphere and normally would not be expected on Iapetus, Titan tholin (or something similar) is a necessary component in our modeling of 5145 Pholus, an object much smaller than Iapetus (Wilson *et al.* 1994). In all cases, poly-HCN or some material with very similar properties is a necessary component for Iapetus.

TABLE I
Inferences Made from Observations of Iapetus

Observation	Inference
1. Albedo contours centered on apex of motion	1. Impacts are important
2. Elliptical contours aligned on equator and bright poles	2. Impactors are mainly from outside the Saturn system
3. Smooth albedo gradient and contours	3. A large number of impacts are required to hide fluctuations (root-N noise)
4. Absence of bright spots deep within Cassini Regio	4a. Darkening occurs much faster than the rate at which craters with diameters just below the limit of Voyager resolution form, or 4b. The dark material is more than several kilometers thick.
5. Some bright spots at the western edge of Cassini Regio	5a. Large impacts somehow inhibit the darkening process, or 5b. The dark material is less than several kilometers thick here, or 5c. The impact flux comes only from the forward direction, allowing backfacing slopes and depressions to be shielded
6. Putative presence of dark-floored craters on trailing hemisphere	6a. Large impacts can produce, directly or indirectly, the necessary conditions for darkening on the trailing hemisphere, or 6b. A global dark layer exists but is covered by ice on the trailing hemisphere

OBSERVATIONAL CONSTRAINTS

In Table I we bring together the main characteristics of the dark material on Iapetus and draw inferences as to their cause. Having the dark material so well centered on the leading hemisphere provides a strong indication that impacts, which will preferentially occur on the leading hemisphere, are key. The elliptical albedo contours aligned with the equator, making the poles the brightest regions on Iapetus, suggest an interplanetary (and not circumsaturnian) origin of the impactors. If dust from Phoebe dominated the flux, the contours would extend closer to the poles (S. Soter, personal communication, 1994; Burns *et al.* 1994), and the antapex would be the brightest region (see Phoebe Dust section below). The smoothness of the contours and the albedo gradient further suggest that a large number of impacts had to occur within each resolution cell of the best Voyager images. If very few impacts were present, then root-N fluctuations would be apparent in the images. And because more than a few percent of exposed bright ice would raise the albedo above what is observed, the dark material is likely to cover >95% of Cassini Regio. Therefore, the surface must be nearly saturated with craters. The impactor size capable of saturation cratering the Iapetus surface can be estimated once a time scale for the cratering/darkening is found.

Depending on the true nature of the dark layer, the distribution of bright- and dark-floored craters on Iapetus will reveal its thickness and/or age. Within most of Cassini Regio, away from its edges where some bright patches are present, there is no clear indication of bright-floored craters. Recent reprocessing of Voyager images, however, do reveal several large low-contrast circular features (Denk *et al.* 1994). It is not yet clear whether these features are due to craters exposing small amounts of bright ice underlying the dark layer, to a difference in surface texture and slope usually associated with fresh craters, or to some other process, so they do not yet provide much insight into the dark layer.

The apparent absence of bright spots then means either (1) the darkening process occurs faster than the rate at which large impacts occur, or (2) the dark material is thick enough that large impacts fail to expose underlying bright material. In conjunction with the constraint that more than a few percent of exposed clean ice would be noticeable in the images, limits can be placed on the dark material thickness, darkening time, and impactor size relevant to darkening. The modern formation rate of craters with $D > 10$ km on Iapetus is $\Gamma_{>10\text{ km}} = 4 \times 10^{-15}$ km^{-2} year^{-1} (Smith *et al.* 1982, Shoemaker and Shoemaker 1990). The best currently available resolution of images of Iapetus is ~20 km/line pair (Smith *et al.* 1982), so a crater 10 km across, exposing bright ice, would be readily apparent against the surrounding dark terrain. The estimated time between 10-km craters forming on the leading hemisphere is ~10^8 years. Unless the dark layer is more than a few kilometers thick, the darkening of the surface—whatever process is responsible—must occur on a time scale faster than this.

Assuming $\Gamma \propto D^{-2.2}$ (Shoemaker and Wolfe 1982), we find that the largest crater expected within each 10-km square pixel in 10^8 years is ~0.1 km, which would not be detectable if it exposed clean ice. The fraction of the surface covered in craters larger than D in 10^8 years is $f \approx 5.5 \times 10^{-4}$ $(D/1\text{ km})^{-0.2}$. Because the power-law distribution breaks down at Earth for meteoroids with $m <$ 100 g (Kyte and Wasson 1986), the minimum D one can use in this expression is ~3 m, giving $f = 0.002$. Therefore, this population of debris is incapable of churning the surface with sufficient frequency and coverage to impose a lower limit on the dark material thickness. In addition, since it does not saturate the surface with impacts, macroscopic debris arriving after the heavy bombardment era cannot be responsible for the dark surface. The important impactor, then, must be interplanetary dust particles with masses ≪100 g. The mass concentration of dust at 10 AU is ~2×10^{-23} g cm^{-3} divided almost equally between two populations with distribution peaks at 10^{-8}–10^{-6} g and 10^{-4}–10^{-2} g (Divine 1993). We estimate an average flux of 1.6×10^{-10} g cm^{-2} year^{-1} impacting Iapetus at 10 km sec^{-1}. Iapetus's orbital motion will increase (decrease) the impact velocity of these particles by ~3 km sec^{-1} at the apex (antapex), resulting in a factor ~2 variation in the impact flux. If it is assumed that the mass is equally divided between 10^{-7} g and 10^{-3} g particles, the surface will be resurfaced to depths of 1–10 mm on time scales of 3000–1.3×10^5 years, respectively. This implies a minimum dark material thickness ~1 cm.

At the western edge of Cassini Regio ~20 small bright spots are present (cf. Burns and Matthews 1986, pp. 908–909, Denk *et al.* 1994). If these features are assumed to be bright-floored craters (smallest diameter ~10 km), they would have had to have formed in the heavy bombardment era. This would appear to rule out the possibility that the darkening process simply occurs so much more slowly at the edges than at the apex that large bright craters survive, since more time has elapsed following the impacts than had preceded them. Instead, the impacts are either (1) inhibiting the darkening process or (2) exposing underlying ice. Since impacts also occurred nearer the apex, it is unlikely the impacts inhibited the darkening process, or else bright spots would be seen all over. Given the higher impact flux at the apex, though, regions of inhibited darkening may have managed to darken anyway. For case (2), the dark layer must be less than a few kilometers thick and thinner at the edges of Cassini Regio than at the apex. Alternatively, (3) these bright patches could be backfacing slopes and depressions shielded from an impact-flux coming almost exclusively from the direction of Iapetus's motion (Bell *et al.* 1985).

Just beyond the western edge of Cassini Regio on the trailing hemisphere of Iapetus there appear to be numerous dark-floored craters. Because of limited phase coverage of this region by Voyager, there exists ambiguity in differentiating dark-floored craters and craters in shadow (Bell *et al.* 1985). If some of these craters are truly dark-floored, this suggests either (4) the darkening process requires large impacts, as opposed to dust impacts, on the trailing hemisphere before darkening can occur or (5) the dark layer extends further into the trailing hemisphere but is covered by a layer of bright ice. Case (4) is incompatible with the idea that large impacts inhibit the darkening process only ~300 km away in Cassini Regio (see previous paragraph). The sizes of the dark craters (~20–200 km) indicate, for case (5), that the dark layer extends to greater depth and is thicker than in the region with the bright spots.

From the preceding discussion, a strong case can be made for a thick, old, global dark layer of varying thickness that is covered on the trailing hemisphere and at the poles by bright ice. One possible surface profile of this layer is shown in Fig. 1. Due to the uncertain identification of dark-floored craters, the figure does not reflect the case of a thicker and deeper dark layer on the trailing hemisphere. Instead, the thickness and depth of the dark layer follow the impact flux contours—a seemingly more reasonable pattern.

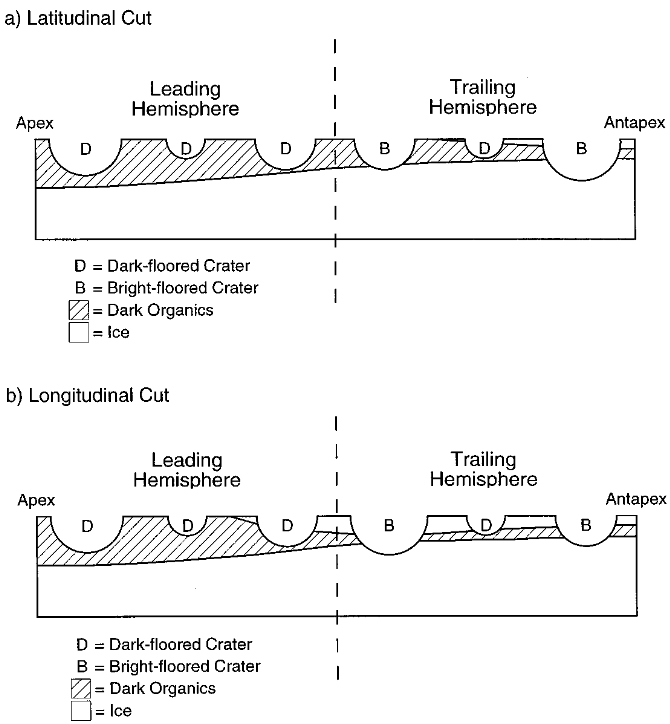

FIG. 1. Schematic surface profiles of ice and organics producing a dark leading hemisphere, a few bright-floored craters at the edges of Cassini Regio, and a few dark-floored craters on the bright trailing hemisphere. The profiles run from the apex to the antapex of motion along (a) the equator and (b) the apex–antapex meridian, passing through the pole. The ice and dark layer thicknesses crudely follow the impact flux contours for interplanetary material. Bright-floored craters within Cassini Regio are produced by impacts that excavate brighter material below the dark layer, and dark-floored craters on the trailing hemisphere are produced when an impact penetrates the surface layer of ice and excavates underlying dark material.

ORIGIN OF DARK MATERIAL AND ALBEDO ASYMMETRY

In light of these possible constraints and the compositions reported above, we now consider each of the seven models proposed for the albedo asymmetry.

Endogenous Extrusion

The principal, and apparently fatal, objection to this hypothesis is the unlikelihood that primordial organics, or organics generated by thermodynamic processes in the interior of Iapetus, should be extruded symmetrically around the apex of orbital motion—much less with photometric contours typical of the impact flux of interplanetary debris. But nothing in the spectrophotometric analysis favoring a composition of HMW (Wilson and Sagan 1995) excludes such an origin. In fact, the analysis may partially support an endogenous origin. It has been proposed that outbursts on comets are driven by the explosive polymerization of hydrogen cyanide, HCN (Rettig *et al.* 1992). If primordial Iapetus were somehow rich in HCN, the exothermic polymerization reaction would have both produced poly-HCN and driven the extrusion process. Murchison organic residue may also be typical of a wide variety of organic solids processed over long periods of time under high temperatures and pressures, as in the Iapetus interior. Indeed, a combined exogenous/endogenous hypothesis may be satisfactory (see below).

Phoebe Dust

There are two major obstacles to the otherwise attractive hypothesis that the Iapetus dark material is impact-ejected from Phoebe, spirals in toward Saturn, and is then collected preferentially on the leading hemisphere of Iapetus. One obstacle is the photometric dissimilarity of the two satellites. Phoebe has an albedo of 0.046–0.060 (Thomas *et al.* 1983) while the darkest region of Iapetus has an albedo ~0.024 (Squyres *et al.* 1984). And from Voyager photometry Phoebe has an OR/VI color of 1.05 while the Iapetus dark material has a color of 1.45 (Squyres *et al.* 1984). Phoebe also has an absorption feature at ~1 μm which is not seen on Iapetus (Tholen and Zellner 1983). Albedo and color, however, vary with particle size and scattering properties, so these arguments are not particularly persuasive. Furthermore, the dust may also change composition during ejection from Phoebe (e.g., by vaporization of the ice) and impact on Iapetus (e.g., by mixing with surface material). In fact, some mixing with the water ice on Iapetus must occur in order to explain the albedo gradient.

It has been suggested that the outermost 0.1–0.5 mm of Phoebe's surface has been heavily processed by cosmic rays while deeper ice remains unaltered (Strazzulla 1986). The bulk of the material transported to Iapetus, then, would not share the observed spectral properties of Phoebe (Strazzulla 1986). The higher processing of Phoebe's surface, however, would make it darker than the underlying ice. But if this underlying ice is the source of the dark material on Iapetus, Phoebe's surface should be darker than Iapetus's. This is not the case.

A second and more formidable obstacle to the Phoebe transfer hypothesis is the photometric contours on Iapetus. Phoebe dust, spiraling in on retrograde orbits, should impact Iapetus's leading hemisphere with some spillover onto the edge of the trailing hemisphere by particles with nonzero eccentricities (S. Soter, personal communication, 1994; Burns *et al.* 1994). The antapex, meanwhile, will be completely shielded from Phoebe particles. Grazing impacts from particles on retrograde orbits requires an eccentricity of 1 or an inclination ~90°. The poles, however, can be hit by any orbit. In fact, because Iapetus has an orbital inclination ~15°, Phoebe dust will be able to reach beyond the poles by approximately this amount. The flux of Phoebe dust at Iapetus's antapex, therefore, should be minuscule compared to the flux near the poles. Whether the low albedo is caused by erosion, deposition, or vaporization, the antapex should clearly be the brightest spot on Iapetus. Instead, Squyres *et al.* find the brightest spot to be near 80° latitude on the trailing hemisphere exactly as predicted by the Cook and Franklin model of the flux of interplanetary particles onto Iapetus. For this reason and, to a lesser degree, because of the difficulties emerging from spectroscopic comparisons, we rule out the Phoebe dust hypothesis.

Reaccreted Ejecta

Similar to the Phoebe dust model, the Tabak and Young (1989) model has Iapetus accreting circumsaturnian material subjected to Poynting–Robertson (P-R) drag. Rather than being particles from Phoebe on retrograde orbits, the dust is Iapetus material put into prograde orbits following a high-velocity comet impact. The heat of the impact vaporizes much of the ice, which would then rapidly dissipate. The material preferentially left in ballistic orbits is the dark involatile component from Iapetus's surface and, to some degree, from the comet.

Tabak and Young (1989) found that material ejected in the direction of Iapetus's motion with a velocity 1.1 times Iapetus's orbital velocity will accrete on the trailing hemisphere for the first 55% of the time during which it crosses Iapetus's orbit. Tabak and Young claim that most of the accretion occurs in the last 45%, during which time it accretes onto the leading hemisphere, because the debris cloud is more diffuse later in its evolution and will encounter Iapetus more efficiently. Assuming a reasonable spread in ejection velocity and direction, though, this is unlikely to be the case. Following an impact, the fraction of ejecta with velocity greater than v scales as v^{-b}, where Tabak and Young take $b = 1.7$. Of the ejecta that can escape Iapetus the fraction with velocity greater than v is $(v/v_e)^{-1.7}$, where $v_e = 0.6$ km sec^{-1} is Iapetus's escape velocity. After escaping Iapetus's gravity well, one-half of the escaping mass will have a velocity relative to Iapetus in the range $0.1v_I$ to $0.4v_I$, with the median mass at $0.2v_I$, where $v_I = 3.3$ km sec^{-1} is Iapetus's orbital velocity. Given the direction of ejection, the orbit of each particle is uniquely determined. In Fig. 2 we follow the evolution of particles ejected from three points on Iapetus: (a) apex; (b) anti-Saturn point; and (c) antapex. Each set of particles is ejected with velocities of $0.1v_I$ and $0.4v_I$ and a directional scatter of $\pm45°$ from the surface normal. After just a couple of orbital periods, the debris trains encircle Saturn and quickly add loops to their spiral. Although early on only a part of Iapetus's orbit intersects the cloud, averaged over the whole orbit the number of particles encountered will be roughly the same as later when the particles have diffused to intersect the entire orbit at all times. Within a few years, then, the ejected debris effectively diffuses to the point

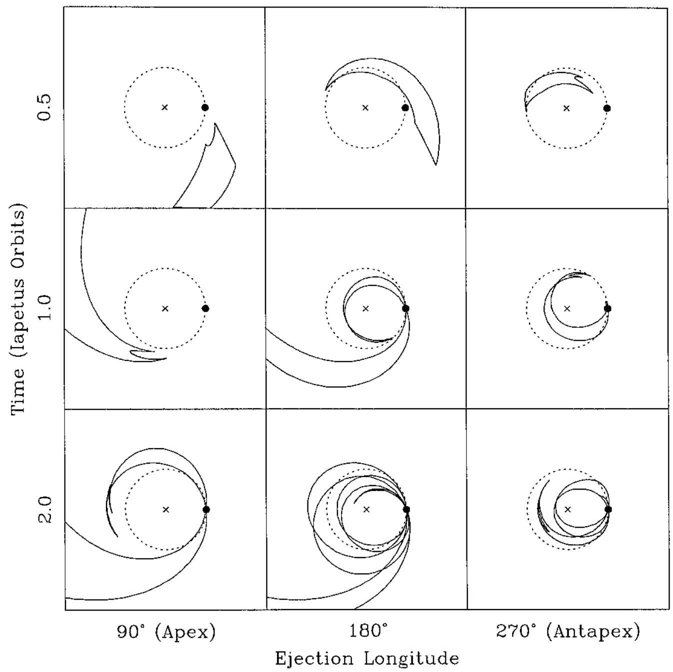

FIG. 2. Evolution of coplanar particles ejected from Iapetus at the apex, anti-Saturn point, and antapex, as seen in Iapetus's corotating frame. The plotted curve connects the set of particles ejected with velocity $0.1v_I$ and $0.4v_I$ and in a direction $\pm45°$ from the surface normal. Iapetus's orbit (dotted circle) and location (small solid circle) are shown. Regardless of ejection direction, after just a few orbits the spread in ejection velocity and direction produces a debris train that encircles Saturn and intersects a significant fraction of Iapetus's orbit. After a few years, the debris train will become so tightly spiraled as to be indistinguishable from a continuous debris cloud.

that it can be treated as a continuous cloud. The gravity of Iapetus and the other satellites, Saturn's oblateness, and radiation pressure will further perturb the particles into ever more-scattered orbits. We, therefore, conclude that reaccretion of ejecta will occur throughout the available time, with accretion decreasing over time as the available material in Iapetus-crossing orbits decreases.

Since the orbits are prograde and may strike anywhere on the satellite given the right semimajor axis, eccentricity, and inclination [all of which vary due to radiation pressure (Burns *et al.* 1979)], it is no simple matter to predict the reaccretion flux contours for the dark material. Initially, though, since all the orbits must pass through the point of ejection, any ejecta from Iapetus will reencounter Iapetus from a direction 180° from the ejection direction. Material can strike anywhere within the hemisphere whose surface normal points in this direction, but for now we care only about the central longitude and latitude. (In fact because of the low encounter velocities, debris captured by Iapetus's gravity will be able to reach a short distance beyond the hemisphere's horizon.) If the orbit is coplanar with Iapetus, material will also accrete at the mirror point about the apex. An impact on the leading hemisphere thus results in an early deposit on the trailing hemisphere, and vice versa. As the Poynting–Robertson effect decreases the semimajor axis of the particles, the particles encounter Iapetus at lower velocities, so accretion occurs closer to the apex. Only when a particle's apoapse passes through Iapetus will accretion occur directly at the apex. Figure 3 shows the evolution of the encounter longitude for coplanar particles ejected in 4 directions with velocity $0.2v_{\mathrm{I}}$ relative to Iapetus. The time for this evolution is given in terms of the orbital decay time due to Poynting–Robertson drag, $\tau_{\text{P-R}}$, which depends on the size and optical properties of the dust; particles with radii ~0.1–0.5 μm evolve fastest with $\tau_{\text{P-R}} \gtrsim 5 \times 10^4$ years (Burns *et al.* 1979). Although for ~1/2 of the time during which it is Iapetus-crossing, forward-ejected debris will accrete on the leading hemisphere (as indicated by Tabak and Young), it does not accrete near the apex except for a very short period towards the end. For ~3/4 of the time, the debris accretes near the limbs, 60° to 120° from the apex. Backward-ejected debris always accretes on the leading hemisphere, but very little time is available before the orbits decay outside the reach of Iapetus.

Debris ejected away from Iapetus's orbital plane will have a relative inclination of ~10°. Initially this material will accrete according to its ejection direction, but unlike debris with coplanar orbits, once the orbit decays a few thousand kilometers it no longer intersects Iapetus's orbit. Therefore, debris in coplanar orbits will dominate the impact flux. Noncoplanar debris is not necessarily unavailable for accretion, though, because solar radiation and orbital precession will continuously alter the relative inclinations

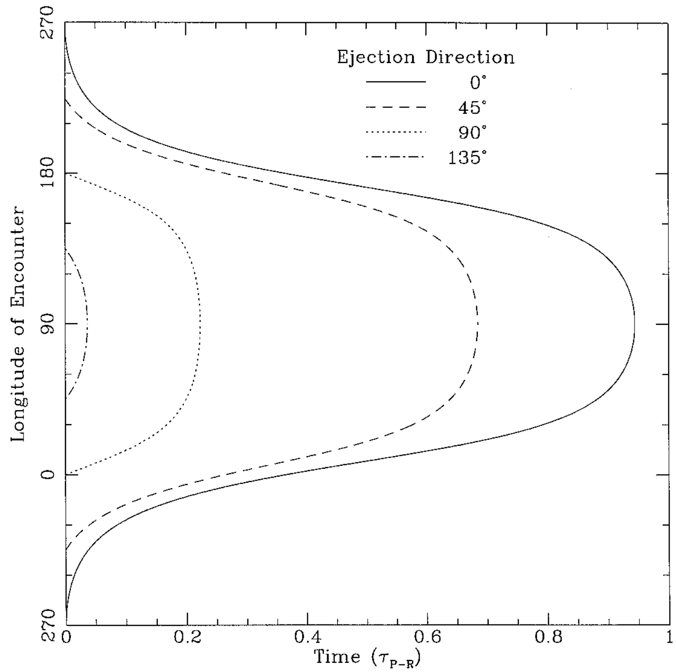

FIG. 3. Evolution of the reaccretion longitude for debris ejected from Iapetus with velocity $0.2v_{\mathrm{I}}$ and affected by Poynting–Robertson (P-R) drag. The ejection direction is measured relative to Iapetus's motion and is parallel to Iapetus's orbital plane. Initially, debris reencounters Iapetus from a direction 180° away from its ejection direction and a mirror point about the apex. As P-R drag decreases the semimajor axes of the orbits, particles encounter Iapetus at slower velocities and the longitude moves toward the apex. Very little time is spent accreting material at the apex, but once the longitude moves to within 60° of it the maximum impact flux will be at the apex because of the overlapping flux from the two mirror points of accretion.

of Iapetus and debris—including debris initially coplanar—on time scales shorter than the decay time of the orbits.

Because coplanar debris from any given direction will have circular accretion flux contours centered at the encounter longitude on the equator, Iapetus's elliptical albedo contours are the result of debris coming from a range of directions. Tabak and Young assumed that the debris accreted only near the apex (or antapex) so they postulated a libration of Iapetus following the impact. Since Fig. 3 shows debris striking away from the apex, librations are not necessary. Indeed because so much time is spent accreting debris at the limbs instead of at the apex, librations are detrimental in many cases; they result in excessive material striking the trailing hemisphere. Because Cassini Regio extends to only ~60° north and south, the impact flux cannot effectively darken a surface more than 60° away from the maximum flux. Accretion of debris then needs to be restricted to longitudes 30°–150°, or else Cassini Regio would be wider than observed. This implies an impact on the trailing hemisphere. If an opening angle of 45° for the escaping ejecta is assumed, the impact needs to occur within 15° of the antapex. Because it will be accreting debris from both the eastern and the western directions, the apex will have the highest impact flux on the satellite despite very little debris coming directly from the zenith.

The volume of debris required to produce a layer $\sim$1 cm thick over 50% of the surface of Iapetus is $\sim 10^{16}$ cm^3. The total volume of ejecta the impact must produce is $(10^{16}\ \text{cm}^3)/\beta\varepsilon\gamma$, where β is the fraction of the ejecta that escapes from Iapetus, ε is the fraction of the debris that is dark material (the rest is assumed to be vaporized ice which is lost), and γ is the fraction of the debris reaccreted. Tabak and Young found $\beta \approx 0.1$ for high-velocity impacts. If an initially bright surface is assumed, the dark material fraction needs to be very small: $\varepsilon \lesssim 0.01$. The comet will contribute some dark material but it will be reduced to its atomic components by the extreme shock temperatures during impact (cf. Chyba *et al.* 1990). It is impossible to obtain a reliable estimate of γ without a detailed simulation which includes all the perturbation sources, but given the short time available for reaccretion, the fraction of material reaccreted is likely to be small: $\gamma \ll 1$. The ejecta volume then needs to be $\gg 10^{19}$ cm^3. Therefore, the minimum crater size is 100 km, which has a volume $\sim 10^{20}$ cm^3. Voyager coverage of the trailing hemisphere, especially south of the equator, is too poor to rule out the presence of a fresh crater this large. North of the equator there are several craters 50–100 km in diameter, but they are closely surrounded by smaller craters, suggesting too great an age.

The formation rate for craters >100 km is 1 every $\sim 6 \times 10^9$ years. To prevent a >10-km crater from penetrating the thin dark deposit, the impact would need to have occurred in the last $\sim 10^8$ years. The probability of such a recent impact is small, but as there are $\sim$10 icy satellites that could have been hit, the probability approaches about 1 in 6. That the impact must occur on the trailing hemisphere is another improbability. The cratering rate for long-period comets varies only by a factor $\sim$3 from apex to antapex (Tabak and Young 1989), so it is not unreasonable for this unique event to occur on the trailing hemisphere. Dust impacts will quickly churn the dark material into the top 1 cm but will not be able to erode away the dark layer for $\sim 5 \times 10^8$ years. At any instant, then, there would be roughly a 1 in 3 chance of finding an Iapetus-like asymmetry somewhere in the Solar System.

Since accretion is being restricted to a narrow range of longitude, the bright patches near the limb can be explained as shadowed slopes (cf. Bell *et al.* 1985). For the same reason, though, it suffers from the same flaws as the Phoebe dust model: it cannot darken the antapex more than the poles. Although the accretion flux is dominated by coplanar debris, some material also will be accreting from low inclination orbits which could encounter Iapetus 30° above and below the equator, extending the flux contours even nearer the poles. One could postulate another recent, but much smaller, impact on the leading hemisphere which would deposit some material on the trailing hemisphere, thereby partially darkening it. Or possibly, we could be seeing the last remnants of a previous large impact on the leading hemisphere $\gtrsim 10^9$ yrs ago being erased by impact erosion. Either of these would make it even more improbable that this series of events would occur and produce an albedo gradient so smooth and continuous. Dark-floored craters on the trailing hemisphere also cannot be explained with this model, but because of the difficulty in distinguishing between dark-floored craters and shadowed crater floors (cf. Bell *et al.* 1985) this failing need not be the model's fatal flaw.

Hyperion Debris

Tholen and Zellner (1983) note that Hyperion is a much better spectroscopic match to Iapetus's leading hemisphere than is Phoebe. This has led to a new model which proposes that Iapetus accreted material ejected from the progenitor of Hyperion when a large, $\sim$100–1000 km, comet struck and disrupted the satellite (Matthews 1992). The similarity between Hyperion and Iapetus is overstated by Matthews (1992) for two reasons, neither of which are serious obstacles for the model, though. First, Hyperion is $\sim$3 times brighter than Iapetus's leading hemisphere (Tholen and Zellner 1983). Second, the Iapetus spectrum showing the strong similarity is contaminated by bright ice at its poles, so the dark material by itself will be both much redder and darker than the Hyperion surface. Both of these problems can be explained by simply claiming a water ice content on Hyperion's surface that is higher than that on Iapetus's leading hemisphere, including the contribution from the poles.

The smallest orbit that is both Hyperion and Iapetus crossing has a semimajor axis 0.7 times Iapetus's and an eccentricity of 0.43. This orbit is only slightly different from the case examined previously for backward-ejected debris from Iapetus. If it is assumed that sufficient material gets put into Iapetus-crossing orbits, then the albedo pattern created will be very similar to that expected from the reaccreted ejecta model. The longitude range over which most of the debris accretes on Iapetus will depend on the velocity distribution of the Hyperion debris, but we expect the range to be similar to the 30°–120° range found earlier. Like the previous two models, the poles will be darkened more than the antapex and there should not be dark-floored craters on the trailing hemisphere.

The spectral similarity between Iapetus and Hyperion seems more likely to be due to ejecta from Iapetus accreting onto Hyperion rather than vice versa. Although the transport of dust from Phoebe to Iapetus is apparently insufficient to influence Iapetus's surface albedo, several factors make the transport of dust from Iapetus to Hyperion more efficient. Most importantly, the ratio of surface areas is much better. Instead of each square cm of Phoebe being spread over 45 cm^2 on Iapetus, the ratio is 25 : 1 for Iapetus to Hyperion, an improvement of a factor of 1000. Second, because Iapetus is nearer Saturn, it will experience a higher impact flux with a higher average impact velocity, thereby producing more ejecta. And third, because of the much lower encounter velocity for dust impacting Hyperion, the dust is more likely to remain on the satellite instead of being reejected into space. Iapetus's higher surface gravity will reduce the flux somewhat but not enough to counter the other three effects. Since Hyperion will be accreting material from both the leading and the trailing hemispheres of Iapetus, Hyperion will have a higher albedo and a color that indicates a mixture of dark material and bright ice, as is seen.

Having found fault with the previous three models for darkening the poles more than the antapex, we now propose a possible solution to this problem. As discussed in the previous sections, impacts on Iapetus will eject material into orbit about Saturn. From our calculations for the reaccretion ejecta model, impacts on the leading hemisphere produce reaccretion deposits on the trailing hemisphere. Once any of the preceding (or following) models produce a dark deposit on the leading hemisphere, that surface will slowly be eroded by dust impacts. Of the small fraction that reaccretes, most of that will impact near 0° and 180° longitude (see Fig. 3). Very little material will accrete at the antapex, but it does not take much dark material to reduce the albedo of a surface from ~0.5 to ~0.3, perhaps as little as ~1% of that eroded from the apex. A detailed numerical treatment of the ejection and reaccretion of debris from Iapetus, including all the perturbation sources, is required before we know if this process is efficient enough to exceed the flux of debris expected at the poles. Until that time, we consider the reacreted ejecta and Hyperion debris models to be only tentatively rejected; the Phoebe dust model has additional photometric problems and remains untenable.

This leaves a class of hypotheses in which photometric contours are expected to follow the flux contours of interplanetary material which are elliptical around the apex, avoid the poles, and have a saddlepoint at the antapex, as observed by Voyager (Squyres and Sagan 1983) and predicted a decade earlier by Cook and Franklin (1970)—because Iapetus is moving through a swarm of interplanetary debris which is on average stationary in Saturn's inertial frame but concentrated along the ecliptic:

Impact Erosion

High-velocity impacts will result in some ejecta escaping Iapetus. Because more impacts occur on the leading hemisphere than on the trailing, the mass loss will be greatest on the leading hemisphere. If a bright surface covers a dark subsurface to a globally uniform depth, the dark subsurface will be exposed first at the apex and then grow as areas of lower flux erode to sufficient depth. The prototypical such hypothesis is that of Cook and Franklin (1970), but Iapetus's low mean density, 1.2 g cm^{-3}, rules out their original suggestion of a silicate mantle being exposed. A generic model in which the dark subsurface is a thin layer (compared to Iapetus's radius) of unspecified origin can explain the observations without requiring a high mean density. Several of the other asymmetry hypotheses can be invoked to produce the dark layer. For example, the organics exposed to view might be a lag deposit or material produced *in situ* (see below). It is also possible that organics uniformly extruded (or accreted) over the entire surface of Iapetus, covered with a thin ice deposit, and preferentially eroded on the leading hemisphere might explain the data. Using Eq. (3) of Cook and Franklin (1970), we estimate an average erosion rate of 20 μm Myr^{-1} for Iapetus. Because of Iapetus's orbital motion, the leading hemisphere has both a higher impact flux and higher impact velocities than the trailing hemisphere, giving an erosion rate that varies from 7 μm Myr^{-1} at the antapex to 36 μm Myr^{-1} at the apex. Therefore, the ice cover would need to be ~10 cm thick to allow, over 3.5 Gyr, erosion on the leading hemisphere to uncover the underlying dark layer while the lower erosion rate on the trailing hemisphere does not. If the ice layer was deposited during the heavy bombardment era, the layer originally could have been as thick as 10 m, assuming a lunar-like time evolution of the dust impact flux (Chyba and Sagan 1992). Even thicker layers are probable since large cometary debris will contribute to the erosion rate in this era.

Lag Deposit

In hypervelocity impacts, some of the kinetic energy will be converted into heat. If the process is efficient, the higher vapor pressure surface materials will preferentially sublimate, leaving behind the more refractory materials (cf. Hartmann 1980). If it is assumed that the amount of ice lost through vaporization is equal to the amount of water ice that can be sublimated by the total conversion of kinetic energy to heat, an upper limit of 15–60 μm Myr^{-1} is found. Combined with the estimate for the physical erosion rate given above, the steady-state concentration of dark material in the deposit can be calculated: Take the top 1 cm of the surface as having a uniform composition of ε dark material and $1 - \varepsilon$ ice overlying material of composition ε_0 dark material and $1 - \varepsilon_0$ ice. At time zero $\varepsilon = \varepsilon_0$. The surface is being physically eroded at a rate δ_e (in μm/Myr), and ice is being vaporized at a rate δ_v. The surface will thus be lost at a combined rate $\delta_e + \delta_v$. In steady state the rate of dark material loss will equal the rate at which dark material is added to the top 1 cm from below: $\varepsilon\delta_e = \varepsilon_0(\delta_e + \delta_v)$. For $\delta_v = 30$ and $\delta_e = 20$ this gives

$$\frac{\varepsilon}{\varepsilon_0} = 1 + \frac{\delta_v}{\delta_e} = 2.5.$$

Since the calculation of δ_v assumed that *all* of the impactors' kinetic energy goes into vaporizing the ice, this is the maximum enhancement possible. Even then an enhancement of a factor of 2.5 in the concentration of dark material is insufficient to convert a bright surface to very low albedo. The erosion rate needs to decrease by a factor ~6 to cause this enhancement factor to increase to ~10, a value closer to that needed for producing a low albedo lag deposit. Since some of the impactors' kinetic energy must go into the ejecta and forming craters in addition to vaporizing ice, an even lower erosion rate than calculated is required. And because the vaporization and erosion rates vary over Iapetus's surface in roughly the same way, the entire surface will be similarly darkened, although the leading hemisphere will darken first. (Having the impacting particles come from Phoebe restricts the darkening to the leading hemisphere but would fail to explain the bright poles and slightly darkened antapex as described in the Phoebe Dust section.) As a currently active process, then, the lag deposit model appears totally inadequate. However, in the early Solar System, when impact rates were much higher and larger impactors saturated the surface with craters, a thick global lag deposit may have formed at the surface, later to be covered by ice. The ice would then have been eroded on the leading hemisphere as in the Cook-Franklin hypothesis.

Compositionally, a lag deposit is consistent with our model. Our best-fit mixtures contain Murchison residue and poly-HCN. The former is of extraterrestrial origin, is expected on C-type and other asteroids, and may well be present on many other bodies in the Solar System. The latter has not been positively identified on any Solar System object, although HCN is present in the Neptunian and Titanian atmospheres (Marten *et al.* 1993; Hanel *et al.* 1981) and is abundant in interstellar clouds (Irvine *et al.* 1987). Also, as mentioned, in modeling 5145 Pholus we find some component with properties similar to poly-HCN to be necessary in all viable models (Wilson *et al.* 1994). The water ice still present can be explained by incomplete devolatilization of the surface, the churning of the surface by the larger impacts, or outgassing and low-temperature deposition at the surface.

In Situ Organic Production

If methane ice or methane clathrate exists on Iapetus's surface (CH_4 is the second most abundant constituent in the atmosphere of nearby Titan), then irradiation by UV photons and high-energy charged particles will convert the mixture to higher hydrocarbons and CHO compounds (cf. Squyres and Sagan 1983, Thompson *et al.* 1987, Khare *et al.* 1989, 1993). Andronico *et al.* (1987) match both Iapetus and Phoebe with pure CH_4 ice irradiated by high-energy ions. At saturnian system temperatures, however, pure methane ice is highly volatile. The vapor pressure at 80 K of methane ice is 20 mbar, which exceeds the hydrostatic pressure $\lesssim$15 m below Iapetus's surface. Therefore, pure methane should be unavailable within the range of any energy sources except decaying radionuclides and very high-energy cosmic rays—which would, however, require $>10^{12}$ years to darken the ice significantly (see below). Moreover, we have compelling observational evidence for abundant water ice on Iapetus (Fink *et al.* 1976, Clark *et al.* 1984), which is expected in any case on cosmic abundance and vapor pressure grounds.

Methane clathrate is stable at these temperatures and the Squyres and Sagan (1983) model for the asymmetry would predict ice tholin—the organic residue from the irradiation of hydrocarbon/water ices—as a major component of the dark material. Although the best model for the dark material does not contain ice tholin, several mixtures with $\chi^2 < 2$ do. Figure 4 plots the best mixtures containing ice tholin for each mixture type. As noted above, poly-HCN and Murchison residue are not unexpected materials, so the HMI intraparticle mixture has nearly as much reason to be expected as HMW—except that the albedo gradient would require us to appeal to a four-component mixture of HMI with water ice. As the absence of water ice allows a better fit at 2.0 μm but a worse fit at 0.4 μm and 1.7 μm, the best four-component

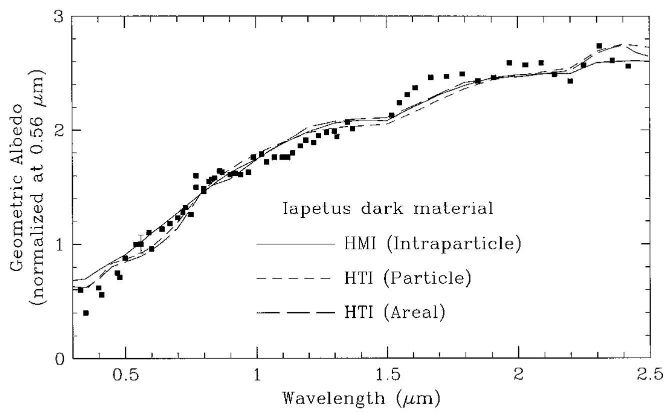

FIG. 4. Comparison of the best Iapetus models containing ice tholin with the dark material spectrum (cf. Fig. 1a of Wilson and Sagan 1995). The mixture containing Murchison residue (HMI) provides a slightly better fit than the Titan tholin mixtures (HTI). In addition, because Titan tholin is produced in an atmosphere while Murchison residue is found in meteorites, the HMI mixture is more reasonable.

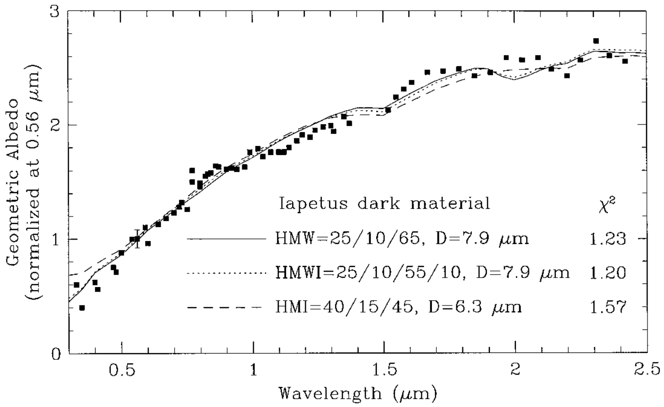

FIG. 5. Comparison of the best intraparticle HMWI mixture with the best HMW and HMI mixtures. The particle size, D, and the reduced chi-squared, χ^2, of each model fit are shown. The Squyres and Sagan (1983) model for the asymmetry predicts ice tholin as a major component in the dark material, but the best three-component composition model (HMW) lacks ice tholin (Wilson and Sagan 1995). However, going to a four-component model that adds ice tholin to the HMW mixture provides an equally consistent fit.

composite model of HMWI is graphed in Fig. 5 and compared to the best HMW and HMI models. HMWI mixtures with up to 15% ice tholin are as consistent with the observations as the HMW model. The Titan tholin in the particle and areal HTI mixtures is less expected than Murchison residue, since it is produced in an atmosphere, although, again, Titan tholin (or something similar) is required in our modeling of 5145 Pholus (Wilson *et al.* 1994). In addition, the particle and areal mixtures have ice tholin only in small (~10%) quantities instead of being the major species as predicted by Squyres and Sagan.

This model has been criticized by Bell *et al.* (1985) on the grounds that it fails to explain the presence of silicates which make up 90% of the Bell *et al.* composition model of the dark material. Because we have shown it is possible to explain Iapetus's spectrum without silicates, this criticism no longer applies.

On Iapetus, the possible sources of irradiation are UV photons ($\lambda < 0.15$ μm), the solar wind, intermittent solar flares, solar and galactic cosmic rays, and the decay of extinct radionuclides. UV photons and the solar wind both penetrate only to ~0.1 μm; solar flares produce energetic particles with energies of 0.1–100 MeV (Lin 1980) which penetrate several centimeters; cosmic rays with energies of many GeV can reach tens of meters beneath the surface; and if distributed uniformly radionuclides will irradiate the entire object. The surface average fluxes of UV, solar wind, and cosmic rays are 0.02 (Chyba and Sagan 1992), 0.01, and ~0.01 erg cm^{-2} sec^{-1} (Thompson *et al.* 1987), respectively. At 1 AU, energetic particles from solar flares reach differential fluxes ~10^{-3} (cm^2 sec sr MeV)$^{-1}$ for 2-MeV particles and scale approximately as E^{-2}, but these high-energy events are active only ~1% of the time (McGuire *et al.* 1986). If it is assumed that the average solar flare particle flux drops with heliocentric distance as r^{-2}, at Iapetus's surface it is ~2×10^{-6} erg cm^{-2} sec^{-1}. If distributed uniformly through the object, the decay of extinct radionuclides delivers, after 4.5 Gyr, a total dose ~10^{11} erg cm^{-3}, the majority of which is deposited in the first few million years by the decay of ^{26}Al (Draganić *et al.* 1984).

A static surface with a hydrocarbon-to-water ratio ~1 : 6 gets converted to complex organic material at the rate $\dot{m} \sim 2 \times 10^{-15}$ g erg^{-1} (Khare *et al.* 1993). The mass fraction of ice converted to organics at an irradiation level, ϕ, is $f = 1 - \exp(-\dot{m}\phi)$. Ten percent of the irradiated layer will be processed and the surface will be significantly darkened when $\phi \approx 5 \times 10^{13}$ erg g^{-1}. The upper 0.1 μm reaches this point in 500 years from the UV and solar wind flux while deeper layers require $>10^{11}$ years of either cosmic ray irradiation or solar flare activity. And unless there are very large inhomogeneities in the concentration of radionuclides, processing by radionuclides is negligible. So, without a process capable of strongly concentrating deeper organics into a lag deposit, only a very thin outer layer exposed to UV photons and the solar wind experiences much *in situ* organic production. That this layer is only ~0.1 μm thick will limit its ability to produce a dark surface at wavelengths $\lambda \gg 0.1$ μm, since these photons will be predominantly scattered by deeper, brighter ice.

Now let us consider the effects of impact gardening. The layer irradiated by UV photons and the solar wind gets mixed into the upper 1 mm on a 3000-year time scale, and into the upper 1 cm on a 1.3×10^5 year time scale. In 500 Myr the upper 1 cm is eroded away. During this time, the top 1 cm will be exposed to on average ~5×10^{14} erg g^{-1} of irradiation, which will process 60% of the ice to ice tholin. For a tholin density ~2 g cm^{-3} and an ice density ~1 g cm^{-3}, tholin will make up ~40% of the surface layer by volume. The impact flux, erosion rate, and ice tholin production efficiency are all probably accurate only to a factor of a few, so the predicted ice tholin concentration could easily be anywhere in the range 10–100 vol%. This range encompasses the 35 vol% total organic concentration in the best model of the dark material as well as the 10 vol% ice tholin content in the best HMWI intraparticle mixture and the particle and areal mixtures. Since the irradiation dose is almost double that at which ice tholin was produced (Khare *et al.* 1993), conceivably some of the ice tholin initially produced is further processed into something spectrally similar to poly-HCN and, especially, Murchison residue (both of which are much more absorbing in the visible than ice tholin).

However, there are several problems with this otherwise promising model. First and foremost, the albedo contours and asymmetry are not directly explained by the impact flux gradient, since the mixing-to-erosion rate should be approximately constant over the entire surface. If the methane concentration is constant over Iapetus's surface, the lower impact flux on the trailing hemisphere means that the ice there should be exposed to higher irradiation levels before being eroded away; the leading hemisphere, conversely, would experience lower irradiation levels than calculated above. An asymmetry opposite to what is observed should, therefore, be seen. A compositional gradient in hydrocarbons and CHO compounds that follows the impact flux gradient—the higher the flux, the higher the organic content—is therefore needed. Deposition of methane-depleted ice on the trailing hemisphere by ballistic diffusion due to the impact gradient has been suggested (Squyres and Sagan 1983). If lateral diffusion of material over large distances were important, though, it should also occur on other airless satellites of similar size and remove all regional albedo contrasts, but this is not the case (e.g., the wispy terrain on Rhea and Dione). And since the amount of ejecta deposited would decrease with distance from the crater, most of the methane-depleted ice would be deposited near the crater, thereby preventing any further darkening. Finally, once the steady-state concentration of organics is reached all of the ejecta should be as dark as the surface.

The second problem with UV/solar wind darkening is that the above estimate of the steady-state organic concentration assumed the maximum hydrocarbon content of methane clathrate ($CH_4:H_2O \sim 1:6$) remaining constant. It is, instead, probable that the top 1 mm will lose some of its volatiles before the surface reaches steady state. Since only $\sim$0.05 μm of ice is converted to dark organics in each 1-mm turnover time, by the 1-cm turnover time this layer will have experienced $\sim$40 impacts, but only have a 0.2 wt% organic concentration. Each impact will shock the layer and fracture the ice particles, releasing some methane gas from its clathrate cage. By the time a 60-wt% organic concentration is reached, the ice will have experienced, assuming the range of fracturing is limited to the physical size of the crater, $\sim$20000 1-mm impacts and $\sim$4000 1-cm impacts. It is unreasonable to assume that this amount of shocking will not affect the methane concentration at the surface. The 10–100 vol% organic concentration is, therefore, only an upper limit for a surface with an initial hydrocarbon-to-water ratio $\sim$1 : 6. In addition, lower initial ratios will have proportionately lower final organic concentrations.

A comparison of the models with the observations is presented in Table II.

THE UNIQUENESS OF IAPETUS

One further discriminant among models may be provided by the question of why Iapetus—alone among satellites of the Saturn system (or indeed, anywhere in the Solar System)—shows such a striking albedo asymmetry. There are mild interhemispheric asymmetries elsewhere in the Solar System, but often in the opposite direction, with brighter leading and darker trailing hemispheres (Veverka 1977). Also the demarcation is not nearly so sharp as on Iapetus. Both Rhea and Dione have orbits interior to Iapetus and should have larger impact fluxes and flux gradients (Shoemaker and Wolfe 1982), but they have brighter leading hemispheres. Dione's asymmetry is larger, with a factor $\sim$1.6 difference between the two hemispheres (Veverka *et al.* 1986) compared to Iapetus's $\sim$5 (Cruikshank *et al.* 1984). Were all other conditions equal, these satellites might be expected to display an albedo asymmetry even more striking than Iapetus's. If the source of the Iapetus dark material were carbonaceous chondritic organics, or something like poly-HCN of interplanetary origin, then many of the objects in the Solar System should have such surface coatings. Likewise, if the hypothetical extruded organic material were common in the deep interiors of many satellites, we would expect to see albedo asymmetries elsewhere, particularly in satellites more massive than Iapetus. On the other hand, if the organic material is produced in a very thin surface layer, bodies with impact fluxes significantly higher and/or irradiation fluxes significantly lower than those of Iapetus may not have enough time to darken before the layer is eroded away or mixed to depth. Or, if a thin ice layer is being eroded, bodies with different impact fluxes and/or ice thicknesses may either have eroded the ice layer globally or not have penetrated the ice layer on the leading hemisphere yet. Alternatively, if a large comet impact resulted in a recent thin deposit of dark debris, the rarity of the event would preclude more than one instance of the asymmetry in the Solar System.

The solution to the mystery of Iapetus's uniqueness seems to involve some compositional anomaly about Iapetus. In fact, Iapetus is near the boundary indicated by thermochemical models of the origin of the Saturn system at which methane clathrate is expected to have condensed out of the circumsaturnian nebula (cf. Pollack *et al.* 1976). Because of the muted spectral signature of CH_4 in low-occupancy methane clathrate (Smythe 1975) and the "self-hiding" aspect of CH_4 in mixed ices (Thompson *et al.* 1987), no contradiction is implied by the apparent absence of CH_4 spectral features on Iapetus. Clearly CH_4 has condensed out at Titan, which is interior to Iapetus. Hyperion, located between Titan and Iapetus, has a nonsynchronous and chaotic rotation (Thomas *et al.* 1984, Wisdom *et al.* 1984), preventing any hemispheric asymmetry from forming. Phoebe shows no significant albedo asymmetry, but because of its retrograde motion, it is thought to be an object captured by Saturn subsequent to the formation of the Saturn system; if it formed in the circumsolar disk it would be CH_4-poor (Prinn 1993). Thus, models which posit processing of methane may be preferred.

TABLE II
Truth Table

Model	Low albedo	Apex darkest	Poles brightest	Smooth and elliptical contours	Bright spots only near edges	Dark spots on trailing hemisphere[a]	Major weaknesses
Endogenous extrusion	Y	N	N	N	?	Y	Unlikely for material to be concentrated at apex with proper contours
Phoebe dust	?	Y	N	Y	Y	N	Antapex should be higher than poles
Reaccreted ejecta	Y	Y	N	Y	Y	N	Unlikely for a suitably large impact to occur near the antapex in the past 10^8 years
Hyperion debris	Y	Y	N	Y	Y	N	Requires ~1 km worth of debris accreted on leading hemisphere but none at pole or antapex
Impact erosion	?	Y	Y	Y	Y[b]	Y[c]	The origin of the dark layer not explained: primordial?
Lag deposit	N	N	N	N	?	?	Insufficient energy in impacts to vaporize enough ice; no asymmetry expected
In situ organics	Y	N	N	N	Y	?	Reverse asymmetry expected
Hybrid: extrusion and impact erosion	Y	Y	Y	Y	Y[b]	Y[c]	Requires two periods of global resurfacing: the first produces a thick dark organic layer, and the second a thin overlying ice layer

[a] Many of these may in fact be shadows (Bell *et al.* 1985).
[b] The dark layer must be more than several kilometers thick at apex and less than this at the western edge of Cassini Regio.
[c] The dark layer must be global and thin enough (or vary in thickness enough) for some craters to completely penetrate the layer on the trailing hemisphere and produce bright-floored craters (see Fig. 1).

The model most capable of producing the observed hemispheric asymmetry is one that proposes a thick layer of organics—be it a lag deposit, extruded material, accreted debris from Iapetus or Hyperion, or irradiated hydrocarbon ices—to be produced no later than shortly after Iapetus's formation, covered by a thin ice deposit, and then excavated on the leading hemisphere by impact erosion. The necessary thickness—a few kilometers—of the dark layer, however, precludes the organics from having formed *in situ* from irradiated methane clathrate and concentrated into a lag deposit, since there does not exist an intense enough radiation source to produce sufficient organic material to avoid requiring the vaporization of hundreds of kilometers of ice. Instead the organic material would need to have been accreted; but then other satellites, regardless of size and composition, should also have accreted organics and formed thick lag deposits, either directly or by reaccretion of ejecta. Since these deposits are not seen, the dark material is unlikely to be of primordial origin. If, instead, the dark material is produced in the interior through thermochemistry and then extruded, the satellite's methane content and, possibly, size will be important in determining how much dark material and ice is deposited on the surface.

It would follow from these ideas that there should be no impact asymmetry in the Jupiter satellite system nor interior to Titan in the Saturn system because the formation temperatures there were too high for significant quantities of methane to be condensed. In the Neptune system, Triton's atmosphere (Stone and Miner 1989) prevents an impact-induced asymmetry from forming because of (1) seasonal ablation and deposition of ice and (2) the shielding of the surface from impactors with $m < 10^{-2}$ g (cf. Bell 1984). Nereid's highly eccentric orbit makes it unlikely to have synchronous rotation (Stone and Miner 1989). In addition, Nereid and the small satellites interior to Triton may be too small to have produced and extruded as much dark material and/or water ice as Iapetus.

The large satellites of Uranus, in contrast to the satellites already dismissed, share most of Iapetus's physical characteristics. They are airless, are similar in size to Iapetus, have synchronous orbits (Smith *et al.* 1986), and should have similar methane contents (Prinn 1993). Thus the absence of an Iapetus-like asymmetry elsewhere in the Solar System seems to follow naturally for models with thermodynamic processing of methane—except for the Uranian satellites.

The reason the Uranian satellites do not share Iapetus's albedo asymmetry, despite the many physical similarities, is explicable because of either higher erosion rates or, despite the expectation to the contrary, lower methane contents in the Uranian system. If the dust flux scales with cometary impacts, the surface of the Uranian satellites will be resurfaced and eroded 2–20 times faster than the surface of Iapetus (cf. Smith *et al.* 1982, 1986; Shoemaker and Shoemaker 1990). Therefore, if a similar amount of ice was deposited on all these satellites, the higher erosion rates in the Uranian system would have completely removed the ice layers on these satellites. And if the circumplanetary nebula from which the satellites formed was in disequilibrium, thereby reducing the quantity of methane collected (Smith *et al.* 1986), the Uranian satellites may have experienced less internal thermochemistry and not have extruded very thick layers of material.

A hybrid model of endogenous extrusion and impact erosion is included in Table II and satisfies all of the observational constraints. Its major weakness is the need to hypothesize two separate periods of global resurfacing. The first produces a thick global layer of dark material on which a thin layer of bright ice is, in a later period, deposited.

CONCLUSIONS AND CONTRIBUTIONS FROM THE CASSINI MISSION

Given the many uncertainties, it is impossible to consider our results as anything approaching conclusive. Nevertheless, an impact erosion model wherein the underlying dark layer is extruded organics conforms best to the range of observational constraints on Iapetus and to the fact that Iapetus is unique in the Solar System. Organic ices and liquids such as methane and ethane have very low densities ($\sim$0.5 g cm^{-3}) and should be present in Iapetus's interior. Radiogenic heat and/or exothermic reactions (e.g., HCN polymerization) will process some of the ices into dark organic materials. With sufficient heating, a mixture of low-density ices, liquids, and gases and denser organic solids ($\rho \approx 2$ g cm^{-3}) can be extruded from the interior of Iapetus. Indeed, the best organic solid/water ice composition found for the dark material (Wilson and Sagan 1995) has a density $\rho \approx 1.3$ g cm^{-3}, which is only slightly higher than Iapetus's bulk density of 1.2 g cm^{-3}. Near the surface, vaporization of the ices and liquids is likely to produce geysers and explosive outbursts, spreading the dark organic/ice mixture over the surface. The source of the overlying ice layer is unclear, but due to its thinness, global extent, and purity, it could be the result of outgassing. After the thermochemistry ceased to be energetic enough to force organics to the surface, the remnant heat would produce water vapor which could escape through fissures and partially condense on the cold surface.

Regarding the other models, *in situ* organic production may work if some mechanism is found to deplete the trailing hemisphere (or enrich the leading hemisphere) of methane. The failure of the lag deposit model appears insurmountable while the various circumsaturnian accretion models seem improbable and/or incapable of producing the proper albedo contours.

Finding a definitive answer will likely depend on a successful Cassini mission. Scheduled to arrive at Saturn in 2004 and remain in orbit for four years, Cassini will carry instruments with much higher spatial and spectral resolution than Voyager's (Sandford 1992). Because it will orbit Saturn, Cassini will be able to map all of Iapetus at 1-km resolution (Murray 1992). During close fly-bys, resolutions better than 100 m are possible (Murray 1992). The best Voyager images of Iapetus have resolutions of only $\sim$10 km (Smith *et al.* 1982). This increase in resolution will have several important implications for the study of the dark material: First, the surface cratering record will be extended to smaller and more abundant impactors, allowing a better characterization of the impact history and regolith turnover rates. Also, as noted above, if the dark layer is relatively thin, large impacts will expose underlying bright material. The Voyager images do not reveal bright spots within most of Cassini Regio, so an upper limit of 10^8 years is set for the darkening time, assuming a thin dark layer. A factor of 10 increase in resolution will decrease this time by over a factor of 100 if no bright craters are seen. If bright craters are seen, the thickness of the dark layer and the rate at which it forms will be directly measurable. Finally, the morphology of the transition region between bright and dark material at all latitudes, as well as the dark-floored craters (if they are real) on the trailing hemisphere and the bright spots at the western edge of Cassini Regio, can be probed. This may indicate independently whether a subsurface dark layer is being exhumed or a once bright surface is being darkened.

The Cassini Visual–Infrared Mapping Spectrometer (VIMS) can observe the wavelength range 0.35–5.1 μm at spectral resolutions of 0.003–0.02 μm with spatial resolution $\sim$1/16 that of the narrow-angle CCD camera (Baines *et al.* 1992, Murray 1992). Since Voyager lacked a near-infrared spectrometer and the infrared spectrum of the dark material used here is only a model calculated from ground-based hemispheric observations, Cassini will provide the first true near-IR spectrum of the dark material. It is conceivable that such high spatial and spectral resolution will usefully constrain the range of possible organic constituents. While it should be difficult to find, as described above, explicit searches for local deposits of methane ice and clathrate are important to attempt. Because of the spatial resolution it will be possible to study how the spectrum changes in going from the apex to the boundary region to the antapex. Spectra of the dark-floored craters can also be isolated and compared to the dark material on the leading hemisphere. Large differences would indicate that different processes produced the two features. Finally, a search for localized darkening processes on Dione and Rhea—which may have retained some CH_4 ice—might be productive.

ACKNOWLEDGMENTS

This research was supported by NASA Grants NAGW 1870 and NAGW 1896. P.W. was supported by the NASA Space Grant program, the NASA Graduate Student Researchers Program, and the Z. Cartter Patten Fellowship at Cornell University. We thank S. Soter, J. Burns, and D. Hamilton for helpful discussions, and J. F. Bell, T. Denk, and an anonymous reviewer for useful comments on this manuscript.

REFERENCES

Andronico, G., G. A. Baratta, F. Spinella, and G. Strazzulla 1987. Optical evolution of laboratory-produced organics: Applications to Phoebe, Iapetus, outer belt asteroids and cometary nuclei. *Astron. Astrophys.* **184,** 333–336.

Baines, K. H., R. H. Brown, D. L. Matson, R. M. Nelson, B. J. Buratti, J. P. Bibring, Y. Langevin, C. Sotin, A. Carusi, A. Coradini, R. N. Clark, M. Combes, P. Drossart, B. Sicardy, D. P. Cruikshank, V. Formisano, and R. Jaumann 1992. VIMS/Cassini at Titan: Scientific objectives and observational scenarios. In *Proceedings, Symposium on Titan* (B. Kaldeich, Ed.), ESA SP-338, pp. 215–219.

Bell, J. F. 1984. Callisto: Jupiter's Iapetus? *Lunar Planet. Sci.* **XV,** 44–45.

Bell, J. F., D. P. Cruikshank, and M. J. Gaffey 1985. The composition and origin of the Iapetus dark material. *Icarus* **61,** 192–207.

Buratti, B. J., and J. A. Mosher 1995. The dark side of Iapetus: Additional evidence for an exogenous origin. *Icarus* **115,** 219–227.

Burns, J. A., D. P. Hamilton, and F. Mignard 1994. The contamination of Iapetus by Phoebe dust. *Bull. Am. Astron. Soc.* **26,** 1160–1161.

Burns, J. A., P. L. Lamy, and S. Soter 1979. Radiation forces on small particles in the Solar System. *Icarus* **40,** 1–48.

Burns, J. A., and M. S. Matthews (eds.) 1986. *Satellites*. Univ. of Arizona Press, Tucson.

Cassini, J. D. 1676. The third satellite of Saturn discovered. *Phil. Trans. R. Soc.* **12,** 831.

Chyba, C. F., and C. Sagan 1992. Endogenous production, exogenous delivery and impact-shock synthesis of organic molecules: An inventory for the origins of life. *Nature* **355,** 125–132.

Chyba, C. F., P. J. Thomas, L. Brookshaw, and C. Sagan 1990. Cometary delivery of organic molecules to the early Earth. *Science* **249,** 366–373.

Clark, R. N., R. H. Brown, P. D. Owensby, and A. Steele 1984. Saturn's satellites: Near-infrared spectrophotometry (0.65–2.5 μm) of the leading and trailing sides and compositional implications. *Icarus* **58,** 265–281.

Cook, A. F., and F. A. Franklin 1970. An explanation of the light curve of Iapetus. *Icarus* **13,** 282–291.

Cruikshank, D. P., J. F. Bell, M. J. Gaffey, R. H. Brown, R. Howell, C. Beerman, and M. Rognstad 1983. The dark side of Iapetus. *Icarus* **53,** 90–104.

Cruikshank, D. P., J. Veverka, and L. A. Lebofsky 1984. Satellites of Saturn: Optical properties. In *Saturn* (T. Gehrels and M. S. Matthews, Eds.), pp. 640–667. Univ. of Arizona Press, Tucson.

Denk, T., R. Jaumann, and G. Neukum 1994. A new search for surface features on the dark leading side of Iapetus. *Bull. Am. Astron. Soc.* **26,** 1163.

Divine, N. 1993. Five populations of interplanetary meteoroids. *J. Geophys. Res. Planets* **98,** 17029–17048.

Draganić, I. G., Z. D. Draganić, and S. Vujošević 1984. Some radiation–chemical aspects of chemistry in cometary nuclei. *Icarus* **60,** 464–475.

Fink, U., H. P. Larson, T. N. Gautier III, and R. R. Treffers 1976. Infrared spectra of the satellites of Saturn: Identification of water ice on Iapetus, Rhea, Dione, and Tethys. *Astrophys. J.* **207,** L63–L67.

Hanel, R., B. Conrath, F. M. Flaser, V. Kunde, W. Maguire, J. Pearl, J. Pirraglia, R. Samuelson, L. Herath, M. Allison, D. Cruikshank, D. Gautier, P. Gierasch, L. Horn, R. Koppany, and C. Ponnamperuma 1981. Infrared observations of the Saturnian system from Voyager 1. *Science* **212,** 192–200.

Hartmann, W. K. 1980. Surface evolution of two-component stone/ice bodies in the Jupiter region. *Icarus* **44,** 441–453.

Irvine, W. M., P. F. Goldsmith, and A. Hjalmarson 1987. Chemical abundances in molecular clouds. In *Interstellar Processes* (D. J. Hollenbach and H. A. Thronson, Jr., Eds.), pp. 561–609. Reidel, Dordrecht.

Khare, B. N., W. R. Thompson, L. Cheng, C. F. Chyba, C. Sagan, E. T. Arakawa, C. Meisse, and P. S. Tuminello 1993. Production and optical constants of ice tholin from charged particle irradiation of (1 : 6) C_2H_6/H_2O at 77 K. *Icarus* **103,** 290–300.

Khare, B. N., W. R. Thompson, B. G. J. P. T. Murray, C. F. Chyba, C. Sagan, and E. T. Arakawa 1989. Solid organic residues produced by irradiation of hydrocarbon-containing H_2O and H_2O/NH_3 ices: Infrared spectroscopy and astronomical implications. *Icarus* **79,** 350–361.

Kyte, F. T., and J. T. Wasson 1986. Accretion rate of extraterrestrial matter: Iridium deposited 33 to 67 million years ago. *Science* **232,** 1225–1229.

Lin, R. P. 1980. Energetic particles in space. *Solar Phys.* **67,** 393–399.

Marten, A., D. Gautier, T. Owen, D. B. Sanders, H. E. Matthews, S. K. Atreya, R. P. J. Tilanus, and J. R. Deane 1993. First observations of CO and HCN on Neptune and Uranus at millimeter wavelengths and the implications for atmospheric chemistry. *Astrophys. J.* **406,** 285–297.

Matthews, R. A. J. 1992. The darkening of Iapetus and the origin of Hyperion. *Q. J. R. Astron. Soc.* **33,** 253–258.

McGuire, R. E., T. T. von Rosenvinge, and F. B. McDonald 1986. The composition of solar energetic particles. *Astrophys. J.* **301,** 938–961.

Melosh, H. J. 1989. *Impact Cratering: A Geologic Process.* Oxford Univ. Press, New York.

Murray, C. D. 1992. The Cassini imaging science experiment. *J. Br. Interplanet. Soc.* **45,** 359–364.

Pollack, J. B., A. S. Grossman, R. Moore, and H. C. Graboske, Jr., 1976. The formation of Saturn's satellites and rings, as influenced by Saturn's contraction history. *Icarus* **29,** 35–48.

Prinn, R. G. 1993. Chemistry and evolution of gaseous circumstellar discs. In *Protostars and Protoplanets III* (E. H. Levy and J. I. Lunine, Eds.), pp. 1005–1028. Univ. of Arizona Press, Tucson.

Rettig, T. W., S. C. Tegler, D. J. Pasto, and M. J. Mumma 1992. Comet outbursts and polymers of HCN. *Astrophys. J.* **398,** 293–298.

Sandford, M. C. W. 1992. The Cassini/Huygens mission and the scientific involvement of the United Kingdom. *J. Br. Interplanet. Soc.* **45,** 355–358.

Shoemaker, E. M., and C. S. Shoemaker 1990. The collision of solid bodies. In *The New Solar System* (J. K. Beaty and A. Chaikin, Eds.), 3rd ed., pp. 259–274. Cambridge Univ. Press, Cambridge.

Shoemaker, E. M., and R. F. Wolfe 1982. Cratering time scales for the Galilean satellites. In *Satellites of Jupiter* (D. Morrison and M. S. Matthews, Eds.), pp. 277–339. Univ. of Arizona Press, Tucson.

Smith, B. A., L. Soderblom, R. Batson, P. Ridges, J. Inge, H. Masursky, E. Shoemaker, R. Beebe, J. Boyce, G. Briggs, A. Bunker, S. A. Collins, C. J. Hansen, T. V. Johnson, J. L. Mitchell, R. J. Terrile, A. F. Cook III, J. Cuzzi, J. B. Pollack, G. E. Danielson, A. P. Ingersoll, M. E. Davis, G. E. Hunt, D. Morrison, T. Owen, C. Sagan, J. Veverka, R. Strom, and V. E Suomi 1982. A new look at the Saturn system: The Voyager 2 images. *Science* **215,** 504–537.

Smith, B. A., L. A. Soderblom, R. Beebe, D. Bliss, J. M. Boyce, A. Brahic, G. A. Briggs, R. H. Brown, S. A. Collins, A. F. Cook II, S. K. Croft, J. N. Cuzzi, G. E. Danielson, M. E. Davies, T. E. Dowling, D. Godfrey, C. J. Hansen, C. Harris, G. E. Hunt, A. P. Ingersoll, T. V. Johnson, R. J. Krauss, H. Masursky, D. Morrison, T. Owen, J. B. Plescia, J. B. Pollack, C. C. Porco, K. Rages, C. Sagan, E. M. Shoemaker, L. A. Sromovsky, C. Stoker, R. G. Strom, V. E. Suomi, S. P. Synnott, R. J. Terrile, P. Thomas, W. R. Thompson, and J. Veverka 1986. Voyager 2 in the Uranian system: Imaging science results. *Science* **233,** 43–64.

Smythe, W. D. 1975. Spectra of hydrate frosts: Their application to the outer Solar System. *Icarus* **24,** 421–427.

Soter, S. 1974. Brightness of Iapetus. Presented at *IAU Colloq.* **28,** Cornell University.

Squyres, S. W., B. Buratti, J. Veverka, and C. Sagan 1984. Voyager photometry of Iapetus. *Icarus* **59,** 426–435.

Squyres, S. W., and C. Sagan 1983. Albedo asymmetry of Iapetus. *Nature* **303,** 782–785.

Stone, E. C., and E. D. Miner 1989. The Voyager 2 encounter with the neptunian system. *Science* **246,** 1417–1421.

Strazzulla, G. 1986. Organic material from Phoebe to Iapetus. *Icarus* **66,** 397–400.

Tabak, R. G., and W. M. Young 1989. Cometary collisions and the dark material on Iapetus. *Earth Moon Planets* **44,** 251–264.

Tholen, D. J., and B. Zellner 1983. Eight-color photometry of Hyperion, Iapetus, and Phoebe. *Icarus* **53,** 341–347.

Thomas, P., J. Veverka, M. Davies, D. Morrison, and T. V. Johnson 1983. Phoebe: Voyager 2 observations. *J. Geophys. Res.* **88,** 8736–8742.

Thomas, P., J. Veverka, D. Wenkert, G. E. Danielson, and M. E. Davis 1984. Hyperion: 13-Day rotation from Voyager data. *Nature* **307,** 716–717.

Thompson, W. R., B. G. J. P. T. Murray, B. N. Khare, and C. Sagan 1987. Coloration and darkening of methane clathrate and other ices by charged particle irradiation: Applications to the outer Solar System. *J. Geophys. Res.* **92,** 14933–14947.

Veverka, J. 1977. Photometry of satellite surfaces. In *Planetary Satellites* (J. A. Burns, Ed.), pp. 171–209. Univ. of Arizona Press, Tucson.

Veverka, J., P. Thomas, T. V. Johnson, D. Matson, and K. Housen 1986. The physical characteristics of satellite surfaces. In *Satellites* (J. A. Burns and M. S. Matthews, Eds.), pp. 342–402. Univ. of Arizona Press, Tucson.

Wilson, P. D., and C. Sagan 1995. Spectrophotometry and organic matter on Iapetus. 1. Composition models. *J. Geophys. Res. Planets* **100,** 7531–7537.

Wilson, P. D., C. Sagan, and W. R. Thompson 1994. The organic surface of 5145 Pholus: Constraints set by scattering theory. *Icarus* **107,** 288–303.

Wisdom, J., S. J. Peale, and F. Mignard 1984. The chaotic rotation of Hyperion. *Icarus* **58,** 137–152.